

Watt-level optical parametric amplifier at 42 MHz tunable from 1.35 to 4.5 μm coherently seeded with solitons

Tobias Steinle,* Andy Steinmann, Robin Hegenbarth, and Harald Giessen

4th Physics Institute and Research Center SCOPE, University of Stuttgart,
Pfaffenwaldring 57, 70550 Stuttgart, Germany

*t.steinle@pi4.uni-stuttgart.de

Abstract: We report on an optical parametric amplifier at high repetition rate of 41.7 MHz seeded by an optical soliton from a tapered fiber. Gap-free signal tuning from 1.35 μm to 1.95 μm with corresponding idler wavelengths from 2.2 μm to 4.5 μm is demonstrated. The system provides up to 1.8 W average power at 1.4 μm , more than 1.1 W up to 1.7 μm , and more than 400 mW up to 4.0 μm with a signal pulse duration of 200 to 300 fs. It is directly pumped by a solid-state oscillator providing up to 7.4 W at 1.04 μm wavelength with 425 fs pulse duration. Soliton-seeding is shown to lead to excellent pulse-to-pulse stability, but it introduces a timing-jitter on the millisecond timescale. Using a two-stage concept the timing-jitter is efficiently suppressed due to the passive synchronization of both conversion stages.

© 2014 Optical Society of America

OCIS codes: (190.4360) Nonlinear optics, devices; (190.4970) Parametric oscillators and amplifiers.

References and links

1. A. Schliesser, N. Picqué, and T. W. Hänsch, “Mid-infrared frequency combs,” *Nat. Photonics* **6**, 440–449 (2012).
2. F. Huth, M. Schnell, J. Wittborn, N. Ocelic, and R. Hillenbrand, “Infrared-spectroscopic nanoimaging with a thermal source,” *Nature Mat.* **10**, 352–356 (2011).
3. A. H. Zewail, *Femtochemistry: Ultrafast Dynamics of the Chemical Bond* (World Scientific, Singapore, 1994).
4. F. Adler, K. C. Cossel, M. J. Thorpe, I. Hartl, M. E. Fermann, and J. Ye, “Phase-stabilized, 1.5 W frequency comb at 2.8–4.8 μm ,” *Opt. Lett.* **34**, 1330–1332 (2009).
5. N. Leindecker, A. Marandi, R. L. Byer, K. L. Vodopyanov, J. Jiang, I. Hartl, M. Fermann, and P. G. Schunemann, “Octave-spanning ultrafast OPO with 2.6–6.1 μm instantaneous bandwidth pumped by femtosecond Tm-fiber laser,” *Opt. Express* **20**, 7046–7053 (2012).
6. S. Marzenell, R. Beigang, and R. Wallenstein, “Synchronously pumped femtosecond optical parametric oscillator based on AgGaSe₂ tunable from 2 μm to 8 μm ,” *Appl. Phys. B* **69**, 423–428 (1999).
7. T. Südmeyer, J. Aus der Au, R. Paschotta, U. Keller, P. G. R. Smith, G. W. Ross, and D. C. Hanna, “Femtosecond fiber-feedback optical parametric oscillator,” *Opt. Lett.* **26**, 304–306 (2001).
8. R. Hegenbarth, A. Steinmann, G. Toth, J. Hebling, and H. Giessen, “Two-color femtosecond optical parametric oscillator with 1.7 W output pumped by a 7.4 W Yb:KGW laser,” *J. Opt. Soc. Am. B* **28**, 1344–1352 (2011).
9. Y.-W. Tzeng, Y.-Y. Lin, C.-H. Huang, J.-M. Liu, H.-C. Chui, H.-L. Liu, J. M. Stone, J. C. Knight, and S.-W. Chu, “Broadband tunable optical parametric amplification from a single 50 MHz ultrafast fiber laser,” *Opt. Express* **17**, 7304–7309 (2009).
10. J. Krauth, A. Steinmann, R. Hegenbarth, M. Conforti, and H. Giessen, “Broadly tunable femtosecond near- and mid-IR source by direct pumping of an OPA with a 41.7 MHz Yb:KGW oscillator,” *Opt. Express* **21**, 11516–11522 (2013).

11. J. Wueppen, B. Jungbluth, T. Taubner, and P. Loosen, "Ultrafast Tunable Mid IR Source," 36th International Conference on Infrared Millimeter and Terahertz Waves (IRMMW-Thz), **1**, 2–7 (2011)
12. C. Erny, K. Moutzouris, J. Biegert, D. Kuhlke, F. Adler, A. Leitenstorfer, and U. Keller, "Mid-infrared difference-frequency generation of ultrashort pulses tunable between 3.2 and 4.8 μm from a compact fiber source," *Opt. Lett.* **32**, 1138–1140 (2007).
13. C. Manzoni, G. Cirmi, D. Brida, S. De Silvestri, and G. Cerullo, "Optical-parametric-generation process driven by femtosecond pulses: Timing and carrier-envelope phase properties," *Phys. Rev. A* **79**, 033818 (2009).
14. M. Marangoni, R. Osellame, R. Ramponi, G. Cerullo, A. Steinmann, and U. Morgner "Near-infrared optical parametric amplifier at 1 MHz directly pumped by a femtosecond oscillator," *Opt. Lett.* **32**, 1489–1491 (2007).
15. G. Cerullo and S. De Silvestri, "Ultrafast optical parametric amplifiers," *Rev. Sci. Instr.* **74**, 1–18 (2003).
16. M. Bradler, C. Homann, and E. Riedle "Mid-IR femtosecond pulse generation on the microjoule level up to 5 μm at high repetition rates," *Opt. Lett.* **36**, 4212–4214 (2011).
17. T. W. Neely, T. A. Johnson, and S. A. Diddams, "High-power broadband laser source tunable from 3.0 μm to 4.4 μm based on a femtosecond Yb: fiber oscillator," *Opt. Lett.* **36**, 4020–4022 (2011).
18. Y. Yao and Wayne H. Knox, "Broadly tunable femtosecond mid-infrared source based on dual photonic crystal fibers," *Opt. Express* **21**, 26612–26619 (2013).
19. J. M. Dudley, G. Genty, and S. Coen "Supercontinuum generation in photonic crystal fiber," *Rev. Mod. Phys.* **78**, 1135–1184 (2006).
20. G. Genty, S. Coen, and J. M. Dudley, "Fiber supercontinuum sources," *J. Opt. Soc. Am. B* **24**, 1771–1785 (2007).
21. A. Steinmann, B. Metzger, R. Hegenbarth, and H. Giessen, "Compact 7.4 W femtosecond oscillator for whitelight generation and nonlinear microscopy," Conference on Lasers and Electro-Optics, OSA Technical Digest (CD) (Optical Society of America, 2011), paper CThAA5.
22. G. P. Agrawal, *Nonlinear Fiber Optics* (Academic Press, San Diego, 1995).
23. S. Pricking and H. Giessen, "Tailoring the soliton and supercontinuum dynamics by engineering the profile of tapered fibers," *Opt. Express* **18**, 20151–20163 (2010).
24. R. Zhang, J. Teipel, X. Zhang, D. Nau, and H. Giessen, "Group velocity dispersion of tapered fibers immersed in different liquid," *Opt. Express* **12**, 1700–1707 (2004).

1. Introduction

Coherent light sources in the molecular "fingerprint" spectral region from 2 - 12 μm are highly attractive since they offer opportunities for spectroscopic experiments on vibrations of molecules and solids. Apart from advantages in terms of precision, sensitivity and recording time compared to thermal sources, near- and mid-infrared lasers are ideal sources for nanoscale imaging, remote sensing and femtochemistry [1–3].

The generation of high-power infrared radiation at *high repetition rate* is mostly dominated by optical parametric oscillators (OPOs) [4–8], while recently also optical parametric amplifiers (OPAs) were shown to provide several hundreds of milliwatts [9, 10]. At higher pulse durations of several picoseconds very efficient optical parametric generation (OPG) was demonstrated [11]. Further, difference frequency generation (DFG) can be employed for mid-IR generation [11, 12].

Compared to picosecond systems, both the higher peak power and the broader spectral bandwidth of femtosecond pulses is beneficial, if spectral information is of interest. Further, a femtosecond pulse can be combined with a spectral filter to narrow the linewidth and increase the pulse duration, while it is much more difficult to achieve this the other way round. Transferring the concept of OPG to the femtosecond regime might encounter problems of intrinsic timing-jitter arising from the quantum-noise seed [13].

In contrast to OPOs, OPAs come with a variety of advantages. They neither require broadband dielectric mirrors nor precise dispersion management and compensation, which results in easy and gap-free tunability. Further, no synchronization of a cavity to the pump laser is needed and therefore OPAs are very robust and simple devices. However, they require a very high single-pass gain in order to reach sufficient conversion efficiencies. The key to achieve competitive output power is to provide enough seed power at the desired wavelength.

In the widely used kHz-systems with regenerative amplifiers or cavity-dumped systems [14] up to 2 MHz, several micro- to millijoule pulse energy are available [15, 16]. This facilitates the

generation of a stable supercontinuum seed in bulk materials such as sapphire, while the high field amplitude makes the frequency conversion very efficient.

In contrast, systems at high repetition rate [10, 17, 18] require nonlinear optical fibers [19] for the seed generation in combination with very efficient nonlinear crystals such as periodically poled lithium niobate (PPLN). However, it has been shown that the coherence of fiber supercontinua decreases significantly if a certain soliton number is exceeded [20]. This effect introduces strong short term pulse-to-pulse fluctuations to the OPA signal. In the following we show that these fluctuations will vanish, if a coherent soliton seed is used, and that the output power can be pushed beyond the Watt-level with a two-stage concept.

2. Experimental setup

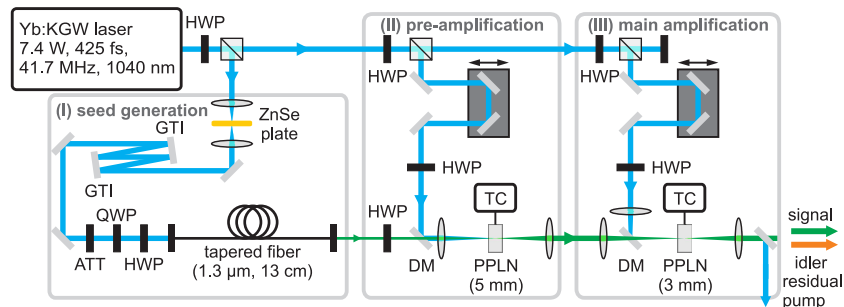


Fig. 1. Experimental setup of the OPA. The seed generation stage (I) includes pulse compression, fiber launch power and polarization control and a small-waist long tapered fiber. The seed is further amplified by two parametric conversion stages (II) and (III). HWP: half-wave plate, QWP: quarter-wave plate, ATT: variable attenuator, GTI: chirped mirror, DM: dichroic mirror, TC: temperature control.

The experimental setup, consisting of a seed generation stage and two successive frequency conversion stages, is shown in Fig. 1. It combines two concepts, namely soliton seeding together with two separate conversion stages, that lead to superior performance compared to supercontinuum-seeded systems. The system is directly pumped by a solitary mode-locked Yb:KGW oscillator [21] with up to 7.4 W average power, 425 fs pulse duration, and 41.7 MHz repetition rate at 1040 nm. For the seed generation, 250 mW are separated and the pulses are spectrally broadened by self-phase modulation in a 3 mm long ZnSe plate. The spot size at the focus is 30 μm in diameter. A pair of chirped mirrors temporally compresses the pulses to 170 fs. The shorter pulse duration is required in order to generate a train of solitons in the subsequent tapered fiber. The 13 cm long tapered fiber with a small core diameter of 1.3 μm is used to generate Raman-red-shifted solitons. Precise alignment of both polarization and launch power turns out to be essential for the stability and shape of the output spectrum. Hence, the input pulse is controlled by a quarter- and a half-wave plate as well as a variable attenuator. The fiber throughput is on the order of 30% and the total fiber output power can be tuned up to 30 mW until damage in the tapered section occurs. The output from this fiber provides a tunable seed up to 1900 nm.

A dichroic mirror (HR 750-1100 nm, AR 1260-1700 nm) combines seed solitons and pump pulses while a delay stage ensures optimum temporal overlap of the pulses. Both beams are overlapped collinearly and focused to a spot size of 40 μm with an achromatic lens with 75 mm focal length into a 5 mm long MgO:PPLN crystal where optical parametric amplification takes place. The spot size of the seed beam turned out to only weakly influence the output signal

beam profile, which is the reason that only one focusing lens was used in this stage. The crystal contains poling periods from $26.5 \mu\text{m}$ up to $31.5 \mu\text{m}$ in steps of $0.5 \mu\text{m}$ and is mounted in an oven that allows for temperature tuning up to 200°C . This stage is pumped with up to 1.4 W pump power. The pump power is decreased to 1.2 W for the $30.5 \mu\text{m}$ period and 1 W for the $31.0 \mu\text{m}$ period in order to avoid damage to the crystal. The signal pulses from this stage are further amplified in a second conversion stage with a 3 mm long PPLN crystal. The AR-coating of the crystals ensures that only small losses of less than 10% are observed if the residual pump power is compared to the generated signal power. A longer focusing length of 150 mm and larger spot size of $80 \mu\text{m}$ allow for higher pump power of the second stage of up to 2.4 W . In order to obtain a proper output beam profile, the mode-matching of the signal from the first and the pump of the second stage is important. Therefore, the spot size of the signal was chosen to match the spot size of the pump beam.

3. Experimental results

The soliton seed spectra are shown in Fig. 2. By varying launch power and polarization, the soliton can be tuned up to 1500 nm while maintaining its typical shape (cf. Fig. 2(a)). While the total fiber output power can be varied up to 30 mW , the power in the leading fundamental soliton, which is used for seeding, stays almost constant at 4 mW with a slightly increasing trend for higher red-shifts. We analyzed the pulse propagation in the tapered fiber by means of numerical simulations of the generalized Nonlinear Schrödinger Equation [19] employing a split-step Fourier-method [22, 23]. According to these simulations, the pulse duration of the solitons is on the order of 50 fs . Figure 2(b) shows that the spectrum can be extended to 1700 nm by changing the launch parameters. The shape of this spectrum can be explained by the group velocity dispersion (GVD) of the tapered fiber [24], which is strongly anomalous from 700 to 1550 nm for $1.3 \mu\text{m}$ taper waist diameter. The dispersion becomes normal at approximately 1620 nm . Hence, the decreasing anomalous dispersion leads to an increasing pulse duration and consequently the red shift of the soliton slows down. Still, there is intensity “leaking” into the normal dispersion regime, which forms the peak observed at 1650 nm .

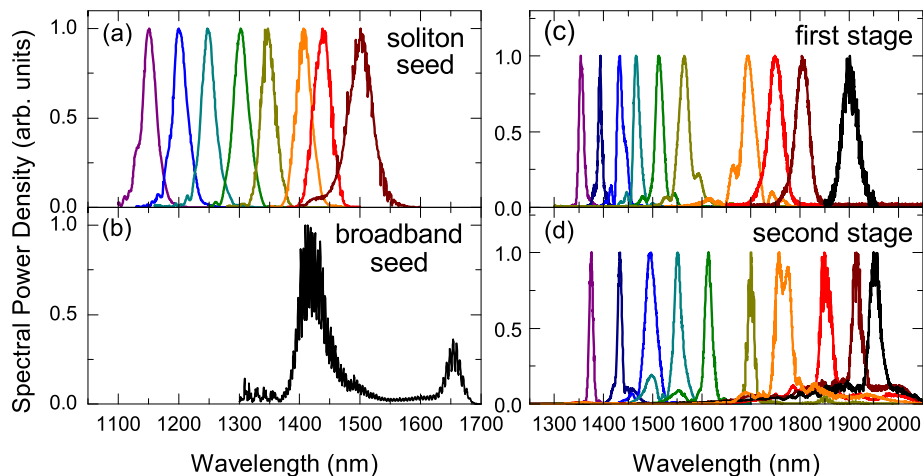


Fig. 2. (a) Tuning spectra of the soliton. For clarity, only the highest order soliton is shown. (b) Broadband seed spectrum obtained with high fiber launch power and polarization alignment. The signal spectra after the first (c) and second stage (d) range from 1.35 to $1.95 \mu\text{m}$. Note that the spectra of each stage are not measured simultaneously.

Further, the formation of fringes in the spectrum can be observed, which is related to a second soliton that follows the leading one. From the fringe distance it can be estimated that the pulse distance is on the order of 1.8 ps, which is reasonable for two adjacent solitons. Due to the outcoupling piece of standard silica fiber (SMF-28) with a total length of 14 cm the pulse is chirped, which can be used for signal tuning by changing the pulse delay. All in all, there is seed power available up to 1900 nm. This spectral range is similar to the spectral range of supercontinua with low coherence [10].

The generated signal wavelengths in the first stage range from 1350 to 1900 nm, which is shown in Fig. 2(c). The pulse duration decreases from 250 to 150 fs with increasing wavelength. All experimentally taken pulse durations relate to the pulse duration of an intensity autocorrelation assuming $sech^2$ pulses. For wavelengths lower than 1500 nm the pulses are almost Fourier-limited while the broad parametric gain bandwidth leads to rather broad spectra above 1500 nm and constant pulse duration of 150 fs up to at least 1600 nm, which is the upper wavelength limit of our autocorrelator. Up to 550 mW signal output power are obtained at 1375 nm, decreasing to 400 mW at 1600 nm and then almost linearly down to 30 mW at 1900 nm as shown in Fig. 3(a). The generated idler is absorbed in the optics between the first and the second conversion stage. All curves that are shown are taken at room temperature and tuning is realized by switching the crystal poling period. Since not all poling periods were available in both crystals due to prior damage, the tuning spectra of the first and the second stage were obtained independently at sub-optimum operation of the first stage. The spectra were chosen to be almost equidistant and then optimized for stability by allowing the wavelength to shift a few nanometers. For fine tuning, the center wavelength of the soliton and the delay between the chirped seed and the pump pulse are changed. This works particularly well for wavelengths above 1500 nm, since the parametric gain bandwidth increases significantly in the spectral region close to degeneracy [15].

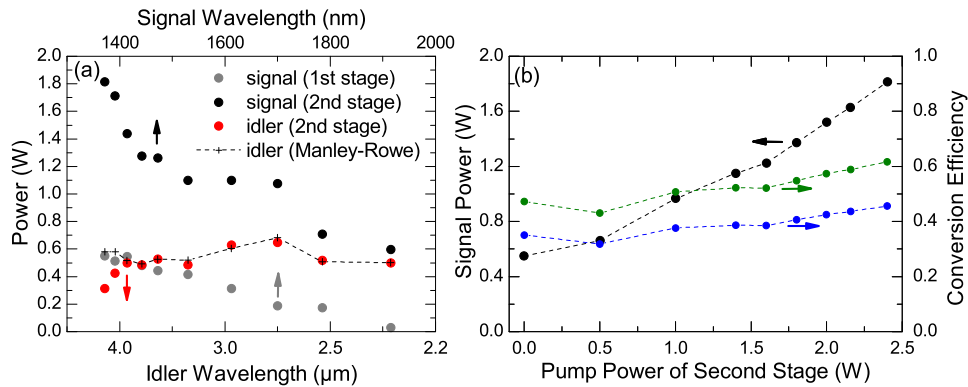


Fig. 3. (a) Signal and idler power versus wavelength. The black dashed line denotes the idler power predicted by the Manley-Rowe relations at the measured signal power. The signal power level of the second stage stays above 1.1 W up to 1700 nm, while more than 400 mW of idler power are generated in the entire tuning range. The decrease of idler power at high wavelengths is due to upcoming absorption in PPLN for more than 4 μm. (b) Total signal power (black) and signal conversion efficiency (blue) of first and second stage versus pump power of the second stage for 1375 nm signal wavelength. The output power (black) increases almost linearly up to 1.82 W, while the signal conversion efficiency increases from 35% to 46%. The photon conversion efficiency (green) reaches more than 61%.

The tuning range of the second stage exceeds the range of the first stage slightly, because it can be seeded by the edge of the seed spectrum of the first stage. Hence, a tuning range from 1350 to 1950 nm center wavelength is observed, as shown in Fig. 2(d). For wavelengths above 1700 nm the onset of OPG is observed which leads to a broad plateau in the spectrum. In principle, the setup can be operated without seed at any wavelength that can be phase-matched, but the stability and output power decrease significantly and spectral properties such as center wavelength and bandwidth can not be influenced by the seed.

In Fig. 3(a) the measured average power of signal and idler over the entire tuning range is shown. The signal power level is greater than 1.1 W in the tuning range up to 1700 nm. For the idler, more than 400 mW are generated in good agreement with the Manley-Rowe relations [15]. The pulse duration after the second stage is typically increased to 200 – 300 fs and the pulses are not at the Fourier-limit anymore. Nevertheless, the autocorrelation is still *sech*²-shaped and does not show wings as known from supercontinuum-seeded systems [10].

Figure 3(b) shows the total signal power at 1375 nm after the second conversion stage versus the pump power of the second stage. Due to the strong seed power from the first stage, which already delivers 550 mW, significant conversion of the pump beam is observed even at low pump powers. Hence, there is only a small dip in the conversion efficiency for 0.5 W pump power, when the second stage does not convert as efficient as the first stage. At a pump power of 1.4 W of the first stage and 2.4 W of the second stage, a maximum signal power of 1.82 W is observed. This value has been measured with a long pass filter with known transmission spectrum and corrected for the filter attenuation. The maximum directly measured power was 1.60 W. Including 0.25 W pump power that is needed for seed generation, the signal conversion efficiency is greater than 45% and the photon conversion efficiency exceeds 60%. This is, to our knowledge, the highest currently measured conversion efficiency of a high-repetition rate OPA-system and competitive in terms of both power and conversion efficiency to currently published OPO-systems [4, 8]. In contrast to OPOs, no customized parts are needed for the entire setup.

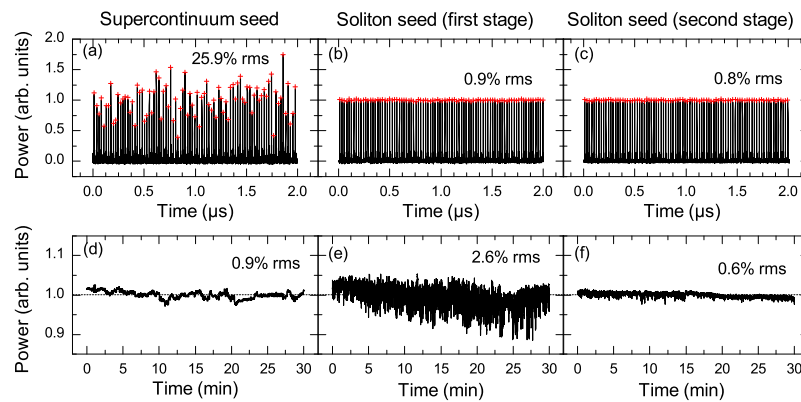


Fig. 4. Noise dynamics on different timescales. (a) Pulse-to-pulse fluctuations of a supercontinuum-seeded OPA [10]. (b) and (c) show the same measurement for a soliton-seeded OPA after the first and second stage. (d)-(f) Long-term stability over half an hour. The measurements were taken at 1550 nm. Better performance is obtained at shorter wavelengths, while the fluctuations increase at higher wavelengths.

One of our main objectives was to overcome the pulse-to-pulse fluctuations that occur in supercontinuum-seeded systems, which would be detrimental for nonlinear spectroscopy experiments. Our measurements are displayed in Fig. 4(a) and taken with a setup of the type as presented in [10]. Hence, a supercontinuum-seeded OPA shows strong pulse-to-pulse fluctuations due to the limited coherence of such supercontinua [20]. Since the soliton number in our system is, depending on the launch power, on the order of 3 to 6, the coherence is maintained and excellent short term stability is observed after both conversion stages, as shown in Figs. 4(b) and (c).

On longer timescales a temporal jitter lowers the stability of the first conversion stage. While Fig. 4(d) demonstrates that the short term fluctuations of the supercontinuum seeded OPA average out on a timescale of seconds, the soliton-seeded OPA shows fluctuations and slight drifts. This is due to a timing-jitter that solitons experience as a consequence of varying launch power. The effect can be understood by investigating the soliton dynamics in the tapered fiber and will be described in the following paragraph.

The soliton red shift, which is due to stimulated Raman-scattering, is intensity dependent. Therefore, less launch power leads to a weaker red shift. On the one hand, this changes the soliton center wavelength very slightly, but on the other hand it also influences the time that the soliton needs for the propagation through the fiber due to its GVD. According to simulations, the delay of the soliton is on the order of $250 \frac{\text{fs}}{\text{mW}}$, which means that very small fiber output power fluctuations on the order of a fraction of a milliwatt significantly influence the temporal overlap of the soliton (pulse duration < 60 fs) with the pump pulse (425 fs). Hence, this timing-jitter leads to large fluctuations in the signal output, where distortions in the operation show up as dips in the output power. The concept of a two-stage setup eliminates this timing-jitter to a certain degree, since the first and the second conversion stage are passively synchronized by the pump beam. Since the conversion in the second stage is strongly saturated, it depends only very weakly on the seed power that is generated by the first stage. Hence, the signal of the second stage is very stable (cf. Fig. 4(f)). The largest share of remaining fluctuations is due to the first stage. However, a strong drift in the soliton may lead to a complete breakdown of the signal power of the first and hence also the second stage. For stable long term operation of more than one hour, slight readjustments of delay or fiber launch power are required. Also, due to the chirped nature of the seed, timing instabilities translate into spectral instabilities which were observed at high signal wavelengths.

4. Conclusion

A high-power femtosecond OPA at 41.7 MHz repetition rate has been demonstrated with a signal tuning range from 1.35 to 1.95 μm and up to 1.8 W average power. The corresponding idler ranges from 2.2 to 4.5 μm , where up to 650 mW average power were obtained. The combination of a coherent soliton seed and two passively synchronized conversion stages lead to power fluctuations of only 0.6% rms over half an hour and excellent short term stability with pulse-to-pulse fluctuations as low as 0.8% rms. Apart from spectroscopic applications, the high output power of this system is well suitable for subsequent nonlinear experiments such as difference frequency generation to extend the spectral range further into the mid-infrared or pumping of nonlinear fibers for mid-infrared supercontinuum generation.

Acknowledgments

We acknowledge financial support from Baden-Württemberg-Stiftung (PROTEINSENS), Deutsche Forschungsgemeinschaft (SPP1391), European Research Council (COMPLEXPLAS), Zeiss-Stiftung, and Alexander von Humboldt Stiftung. This work was supported by the German Research Foundation (DFG) within the funding program Open Access Publishing.